

# A Modified Approach in Modeling and Calculation of Contact Characteristics of Rough Surfaces

J.A. Abdo\*

Mechanical and Industrial Engineering Department, College of Engineering, Sultan Qaboos University, P.O. Box 33, Al-Khod 123, Muscat, Sultanate of Oman

Received 10 November 2003; accepted 30 July 2004

## نموذج رياضي معدل لحساب خصائص التماس للاسطح الخشنة

**المستخلص:** هذه الورقة تقدم نموذج رياضي لقياس الاسطح الخشنة. اشتقاق المعادلات الرياضية تم من خلال تعريف النتوات غير المرنة والتي يفترض ان تتداخل الى حد معين في سطح النتوات الحقيقي. سطح النتوات يفترض أن ينحني بشكل مرن بينما النتوات غير المرنة تنحني بشكل غير مرن بحيث يتبع قانون حفظ الحجم. لهذا البحث افضلية لسببين: (أ) يعطي دقة أكبر لحساب سلوك تماس السطح المرن وغير المرن. (ب) قابل للتطبيق والاستعمال في ايجاد معادلات التماس الجانبي. يقدم البحث ايضا مقارنة عددية لتقدير المساحة والقوى الحقيقية للتماس بين الناتج من استخدام هذا النموذج الرياضي ونتائج دراسات اخرى تمت سابقا.

**المفردات المفتاحية:** التماس المرن-غير المرن، الاحتكاك، الاسطح الخشنة، نموذج رياضي للتماس.

**Abstract:** A mathematical formulation for the contact of rough surfaces is presented. The derivation of the contact model is facilitated through the definition of plastic asperities that are assumed to be embedded at a critical depth within the actual surface asperities. The surface asperities are assumed to deform elastically whereas the plastic asperities experience only plastic deformation. The deformation of plastic asperities is made to obey the law of conservation of volume. It is believed that the proposed model is advantageous since (a) it provides a more accurate account of elastic-plastic behavior of surfaces in contact and (b) it is applicable to model formulations that involve asperity shoulder-to-shoulder contact. Comparison of numerical results for estimating true contact area and contact force using the proposed model and the earlier methods suggest that the proposed approach provides a more realistic prediction of elastic-plastic contact behavior.

**Keywords:** Elastic-plastic, Contact, Friction, Rough surfaces, Contact model

## 1. Introduction

Many engineering problems lead to the consideration of contact between surfaces. These include studies related to friction-induced vibration and noise, thermal and electrical contact resistance, and mechanical seals, bushing, fasteners, etc. Examination of contact characteristics encompasses equivalent contact stiffness and damping for vibration and noise, and true contact area for mechanical seals, and electrical and thermal resistance. Accounting for contact characteristics inherently necessitates characterization of surface topography and development of probabilistic models, which relate contact area, contact stiffness, contact load and separation of surfaces.

These models are based on the presumption that a surface can, in effect, be represented by a distribution of asperities. As two surfaces are brought into contact, the macroscopic contact characteristic in question is a cumulative effect of localized interactions of the asperities. This approach has required the statistical formulation of a surface and statistical summation of microscopic contact effects to obtain probabilistic macroscopic expectation of

the contact characteristic (contact area, load, and stiffness).

Greenwood and Williamson (1966) pioneered "asperity-based model." The existing literature shows extensions of the Greenwood and Williamson (GW) model over the last three decades. The present probabilistic models of contact may be viewed with respect to the premise of elastic and plastic contact. The elastic models primarily rely on the Hertz theory of contact between two elastic bodies (Greenwood and Williamson, 1966; Greenwood and Tripp, 1967, 1970; Hisakado, 1974; Bush *et al.* 1975 and McCool, 1966). These models differ in their assumptions related to surface and asperity geometry and material properties. These extensions have included, for instance, the inclusion of the surface curvature effects Greenwood and Tripp, (1967), allowance for non-uniform curvature of asperity summits Hisakado, (1974) and presumption of average elliptic paraboloidal representation of asperity Bush *et al.* (1975). Other works presented advanced models for anisotropic materials McCool, (1986). Of particular interest to the future goal of the present work is the surface model in which asperities are allowed to form contact on shoulders Greenwood and Tripp, (1967). The plastic models are based on the presumption that

\*Corresponding author E-mail: jdabdo@squ.edu.om

contact is dominated by plastic flow. Such models may be best suited for load ranges that warrant large degree of plastic flow. The earliest work on plastic contact model is attributed to Abbott and Firestone (1933). This model utilizes the geometrical intersection of a plane with a rough surface and presumes that contact flow pressure exists over the area of contact, obtained from geometrical intersection. Later works include two dimensional random process model Nayak, (1971), and investigations leading to the postulation that volume conservation dictates plastic flow (Pullen and Williamson, 1972; Nayak, 1973). The research work of Francis (1976, 1977), dealing with plastic deformation of contact, include empirical characterization using the results for spherical indentation. Liu *et al.* (2000) derived exponential functions from a fitting procedure applied to numerical results of the Gaussian height distribution offering analytical expression for the Greenwood and Williamson (1966); elastic model, Chang, *et al.* (1986), elastic-plastic model and Horng, (1998) elliptic elastic-plastic model.

Whereas the elastic and plastic models are seen to be advantageous for extreme cases of loading, in a large number of engineering applications, contact loads may fall within ranges that do not warrant adequate representation by either elastic or plastic model. This fact has led researchers to consider what is referred to as elastic-plastic models (Ishigaki *et al.* 1979, Chang *et al.* 1997). In the latter work, elastic-plastic model of contact is proposed based on the conservation of volume during plastic deformation. The work proposed by Chang *et al.* (1997) treat contact as elastic-plastic at macroscopic scale while at microscopic level it views an asperity to experience initially elastic deformation followed by purely plastic deformation when a critical interference is reached. More recent works (Kucharski *et al.* 1994; Chang, 1986) have

considered and modified contact models to treat elastic-plastic behavior of metallic coating.

Finite element method solutions to elastic-plastic contact problems were also utilized. Liu *et al.* (2000) developed a finite element method solution for an elastic-plastic contact problem. The finite element method presented by Kogu and Etsion (2002) suggested that the evolution of the elastic-plastic contact could be divided into three distinct stages. Kogu and Etsion (2003) presented an improved finite element-based model for the contact of rough surfaces. The contact parameters for a single asperity contact were predicted.

The present work proposes a modified elastic-plastic model for surfaces in contact. The critical interference proposed by Chang *et al.* (1986) is utilized to define fictitious asperities. In this manner two sets of asperities are defined: (1) those that are the actual surface asperities and (2) the fictitious asperities which can only deform plastically. The concept of elastic and plastic asperities allows formulation of asperity deformation model which is also elastic-plastic at microscopic scale; in contrast to the model by Chang *et al.* (1986). Volume conservation is applied only to the plastic (fictitious) asperities. Comparisons of the contact load/separation values predicted by the proposed model with that obtained through experiments as reported by Kucharski *et al.* (1994) demonstrate the effectiveness of the method in providing accurate prediction of contact characteristics.

## 2. The Mathematical Model

Consider first the contact between a rough surface covered with a number of asperities, that have spherical shape at their summits with average radius  $R$  and a nominally flat surface shown in Fig. 1. The summit heights,  $z$ , are

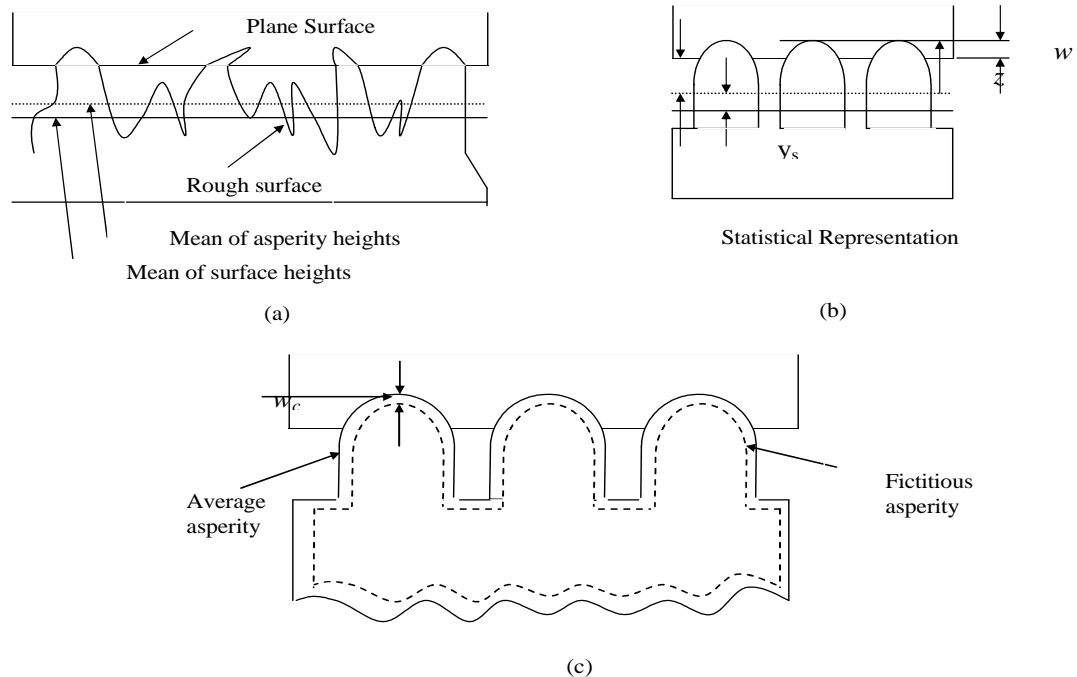


Figure 1. Contact between a flat and a rough surface

assumed to have probability density function  $\phi(z)$ . The probability that an asperity develops contact with the flat plane is (Greenwood and Williamson, 1966):

$$\text{Prob}(z > d) = \int_d^{\infty} \phi(z) dz \quad (1)$$

where  $d$  is the separation based on asperity heights. For  $N$  asperities, the expected number of contacts will be:

$$N_c = N \int_d^{\infty} \phi(z) dz \quad (2)$$

where the total number of asperities,  $N$ , the density of asperities,  $\eta$ , and the nominal area,  $A_n$ , are related according to

$$N = \eta A_n \quad (3)$$

For this type of contact, the interference  $w$  may be described as (Greenwood and Williamson, 1966):

$$w = z - d \quad (4)$$

In analyzing the contact, the laws describing the dependence of the local contact area,  $A_o$ , and the local contact load,  $P_o$ , on  $w$  are employed. Hence,

$$A_0 = A_0(w), \quad P_0 = P_0(w) \quad (5)$$

The expected total contact area,  $A_l$ , and the expected total contact load,  $P$ , are the statistical sums of the local contributions of each asperity. Therefore,

$$A_l(d) = \eta A_n \int_d^{\infty} A_0(z-d) \phi(z) dz \quad (6)$$

$$P(d) = \eta A_n \int_d^{\infty} P_0(z-d) \phi(z) dz \quad (7)$$

The Hertzian contact area,  $A_o$ , contact load,  $P_o$ , and the maximum contact pressure between one asperity, having interference  $w$  with a plane,  $P_m$ , are given as follows:

$$A_0 = \pi R w \quad (8)$$

$$P_0 = \frac{4}{3} E R^{1/2} w^{3/2} \quad (9)$$

$$P_m = \frac{3}{2} \frac{P_0}{A_0} = \frac{2E}{\pi} \left( \frac{w}{R} \right)^{1/2} \quad (10)$$

where,

$$\frac{1}{E} = \frac{1-\nu_1^2}{E_1} + \frac{1-\nu_2^2}{E_2} \quad (11)$$

In the equations above  $R$  is the average equivalent radius of curvature. In general, the maximum contact pressure is related to the hardness of the softer material,  $H$ , through

$$P_m = KH \quad (12)$$

where  $K$  is the maximum contact pressure factor. Tabor (1977) showed that the plastic flow is reached when  $P_m = 0.6H$ . The critical interference at the inception of plastic deformation  $w_c$  is defined by substituting Eq. (12) in Eqs. (10) and (14).

$$A_0 = \frac{\pi a^2}{4} = \pi R w \left( 2 - \frac{w_c}{w} \right) \quad (13)$$

For  $w > w_c$ , the contact is plastic. Using the critical interference and imposing the conservation of volume, Chang *et al.* (1997) derived the modified equations describing the contact area and load on an asperity:

$$A_0 = \frac{\pi a^2}{4} = \pi R w \left( 2 - \frac{w_c}{w} \right) \quad (14)$$

and

$$P_0 = \pi R w \left( 2 - \frac{w_c}{w} \right) KH \quad (15)$$

It is appropriate here to emphasize the difference between the present work and that proposed by Chang *et al.* (1997). In the derivation of the equations, the authors assume that an asperity behavior is initially elastic. As the load is increased the elastic behavior continues to describe the deformation until a critical interference is reached. At this critical load and beyond, the asperity deforms as a purely plastic body. In the work of Chang *et al.* (1997) the elastic and plastic behavior do not occur simultaneously for an asperity. Hence, their formulation can only be characterized as an elastic-then-plastic model at microscopic scale.

The method proposed in this paper is shown to represent more accurately an elastic-plastic model of the contact, through the introduction of a fictitious surface that can only deform plastically. As shown in Fig. 1, the critical interference,  $w_c$ , is used to define a second surface. This second surface is obtained by displacement of every point on the surface by  $w_c$  along the direction normal to the surface (see Fig. 2). As illustrated in Fig. 2, to obtain the mathematical description of the plastic asperity, the mapping of a point, A, on the surface to a point, B, on the plastic asperity must be considered. It is also noted that an asperity is described Fig. 2 in terms of a frame of reference whose origin is at the asperity peak and ordinate points towards the mean plane Greenwood and Tripp, (1967). Therefore,  $\rho y$ -frame is used to describe the original asperity, whereas,  $xy$ -frame is employed for the plastic asperity.

The respective positions of points A and B are denoted by  $\bar{r}_A$  and  $\bar{r}_B$ , as depicted in Fig. 2. The position of point B on the fictitious asperity is :

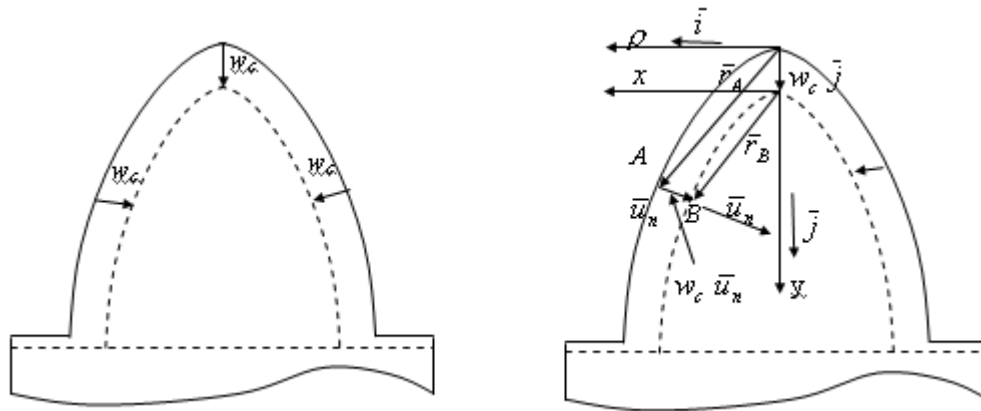


Figure 2. Plastic (fictitious) asperity shape

$$\bar{r}_B = -w_c \bar{j} + \bar{r}_A + w_c \bar{u}_n \tag{16}$$

where,  $\bar{u}_n$  is the unit normal vector to the original asperity at point A. As usual, the unit vectors  $\bar{i}$  and  $\bar{j}$  are defined along  $\rho$  (or  $x$ ) and  $y$  axes, respectively. Employing the notation of Greenwood and Tripp (1967),

$$\bar{r}_A = \rho \bar{i} + \frac{1}{2R} \rho^2 \bar{j} \tag{17}$$

Equations (16) and (17) may be used to obtain the equation describing the plastic asperity (see Appendix A for detail). To the first approximation, the equation of the plastic asperity is given as (Appendix A):

$$y = \frac{x^2}{2(R - w_c)} \tag{18}$$

Since the plastic asperities only deform plastically, their introduction allows the reduction of Eqs. (14) and (15) to the well-known forms:

$$A_0 = 2\pi R_p w \tag{19}$$

$$P_0 = 2\pi KHR_p w \tag{20}$$

Where,  $R_p$  represents the summit radius of curvature of the plastic asperity. Based on Eq. (18), this radius of curvature is

$$R_p = (R - w_c) \tag{21}$$

Clearly the formulation of the area of contact and contact force for two surfaces involves interactions of two sets of asperities: the original surface asperities which are assumed to deform elastically and plastic asperities that deform plastically. The next section presents this new mathematical model of contact.

### 3. Elastic-Plastic Contact Between a Rough Surface and a Plane

The contact between one asperity on a rough surface and a plane is considered. Figure 3 illustrates two types of interactions. The first is the elastic contact between the plane and the surface asperity. If the interference,  $w$ , exceeds the critical interference  $w_c$ , then the interaction also includes plastic contact. It is noted that the shaded volume representing the interference of the plastic asperities and the plane contribute to the plastic portion of contact whereas the remaining volume of interference contributes to the elastic contact. Therefore if we let  $Q$  be the characteristic of contact (area or load) then it may be obtained by appropriately accounting for the aforementioned interactions, that is:

$$Q = Q_{e1} - Q_{e2} + Q_{p2} \tag{22}$$

where  $Q_{e1}$  corresponds to the elastic contact between the plane and surface asperity. However this includes, as shown in Fig. 3, a portion of the interference which is plastic. Therefore, the contribution due to elastic interfer-

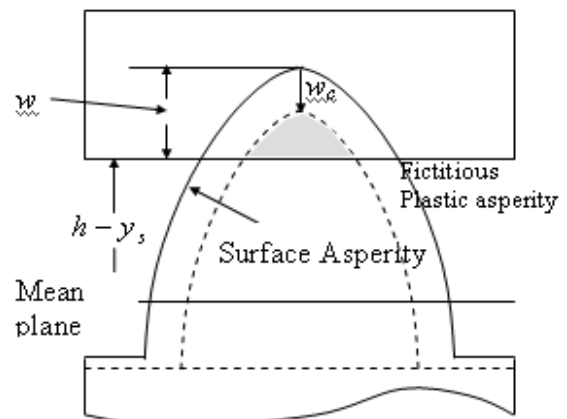


Figure 3. Elastic-plastic interaction of an asperity with a plane

ence between the plane and the plastic asperity  $Q_{e2}$  must be subtracted to obtain the net elastic contribution. The contribution from plastic interaction due to the plastic interference of the plane and plastic asperity  $Q_{p2}$  is, then, added to the result. Using this approach the area of contact may be described as:

$$A_t^*(h) = A_{e1}^* + A_{p2}^* - A_{e2}^* \quad (23)$$

where,

$$A_{e1}^*(h^*) = \pi\beta \int_{h^* - y_s}^{\infty} w^* \phi(s) ds \quad (24)$$

$$A_{e2}^*(h^*) = \pi\beta_p \int_{h^* - y_s + w_c}^{\infty} w^* \phi(s) ds \quad (25)$$

$$A_{p2}^*(h^*) = 2\pi\beta_p \int_{h^* - y_s + w_c}^{\infty} w^* \phi(s) ds \quad (26)$$

where  $\phi(s)$  is the dimensionless form of the probability density function for summit height distribution.  $\beta$ ,  $\beta_p$ ,  $w^*$  and the dimensionless height of asperity,  $s$ , are defined as follows:

$$\beta = \eta R \sigma, \quad \beta_p = \eta(R - w_c) \sigma \quad (27)$$

$$w^* = s - h^* + y_s \quad (28)$$

$$s = \frac{z}{\sigma} \quad (29)$$

It is noteworthy to mention here that the plastic asperity peaks can be viewed as being farther away from the plane by  $w_c$ . We have made the approximation as to the mean plane of plastic asperity being  $w_c$  below the mean plane of the surface asperities. Therefore the limits of integration are shifted by  $w_c$  as presented in Eqs. (25) and (26). Furthermore, in these equations the summit curvature corresponding to plastic asperities are used. Proceeding in a similar manner, the contact load may be written as:

$$P^*(h^*) = P_{e1}^* + P_{p2}^* - P_{e2}^* \quad (30)$$

where,

$$P_{e1}^*(h^*) = \frac{4}{3} \left( \frac{\sigma}{R} \right)^{1/2} \beta \int_{h^* - y_s}^{\infty} w^{*3/2} \phi(s) ds \quad (31)$$

$$P_{e2}^*(h^*) = \frac{4}{3} \left( \frac{\sigma}{R} \right)^{1/2} \beta_p \int_{h^* - y_s + w_c}^{\infty} w^{*3/2} \phi(s) ds \quad (32)$$

$$P_{p2}^*(h^*) = 2\pi K \frac{H}{E} \beta_p \int_{h^* - y_s + w_c}^{\infty} w^* \phi(s) ds \quad (33)$$

## 4. Results: Evaluation of the Proposed Model

The effectiveness of the proposed model is evaluated using the data and results given by Chang *et al.* (1997) and Kucharski *et al.* (1994). For convenience we shall refer to the former as CEB and the latter as KKPK models. The proposed model in this paper will be referred to as AFM model. In the ensuing discussion, results are presented in two subsections. In the first subsection the AFM model is evaluated and compared with the CEB model. In the second subsection AFM, CEB and KKPK models are tested against experimental results given by Kucharski *et al.* (1994).

### 4.1 Comparison of AFM and CEB models

In the CEB model, as it is the case in our model, a dimensionless form of the probability density function is introduced:

$$\phi^*(s) = (2\pi)^{-1/2} \left( \frac{\sigma}{\sigma_s} \right) \exp[-0.5 \left( \frac{\sigma}{\sigma_s} \right)^2 s^2] \quad (34)$$

To combine the material and surface topographic properties in contact, the plasticity index,  $\psi$ , is introduced according to Greenwood and Williamson (1996):

$$\psi = \left( \frac{w_c}{\sigma_s} \right)^{-1/2} \quad (35)$$

The relation between separation  $h$  and  $\sigma$  of the surface microgeometry model and  $d$  and  $\sigma_s$  of the asperity-based model is given as:

$$\sigma^2 = \sigma_s^2 + \frac{3.717 \times 10^{-4}}{\eta^2 R^2} \quad (36)$$

A form for plasticity index is obtained by substituting Eqs. (13) and (36) in (35), to give:

$$\psi = \frac{2E}{\pi KH} \left( \frac{\sigma}{R} \right)^{1/2} \left( 1 - \frac{3.717 \times 10^{-4}}{\beta^2} \right)^{1/4} \quad (37)$$

The data employed by Chang *et al.* (1997) pertaining to steel on steel material is employed with the following parameters:  $E_1 = E_2 = 2.07 \times 10^5 \text{ MPa}$ , Brinell hardness  $H = 1960 \text{ MPa}$ ,  $\nu_1 = \nu_2 = 0.29$ . The maximum contact pressure is taken to be based on  $K = 0.6$ , and  $\beta$  and  $\sigma/R$  are selected for different values of plasticity index from the experimental work of Nuri and Halling (1975).

These values and the values of  $w_c^*$  and  $\sigma/\sigma_s$ , calculated from Eqs. (35) and (36), respectively, are shown in Table 1. Figure 4 illustrates the contact area versus separation, both given in dimensionless form, for the AFM and CEB models. While both models predict similar contact area for low plasticity index, the AFM model predicts higher values for materials of higher plasticity index. Figure 5 depicts the dimensionless

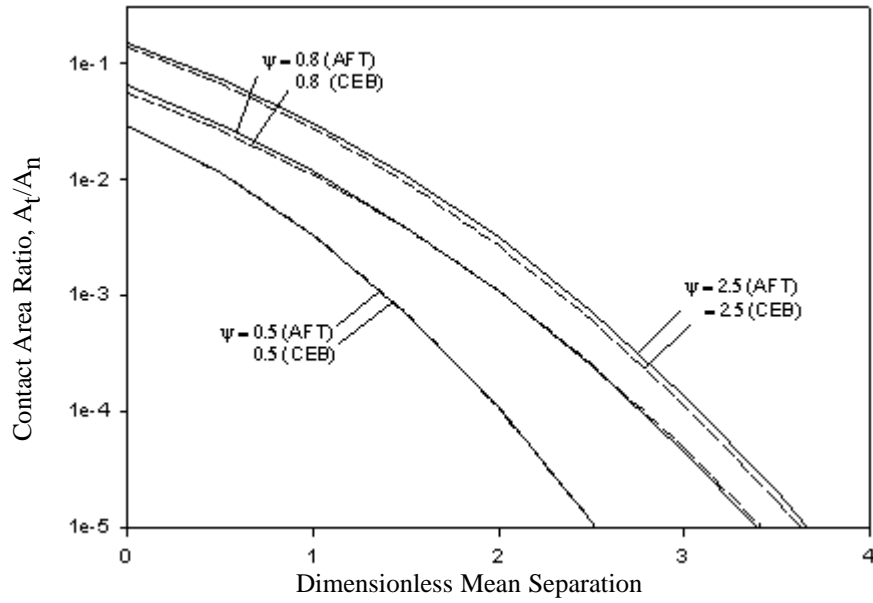


Figure 4. Contact area ratio versus separation: Comparison between AFT and CEB models

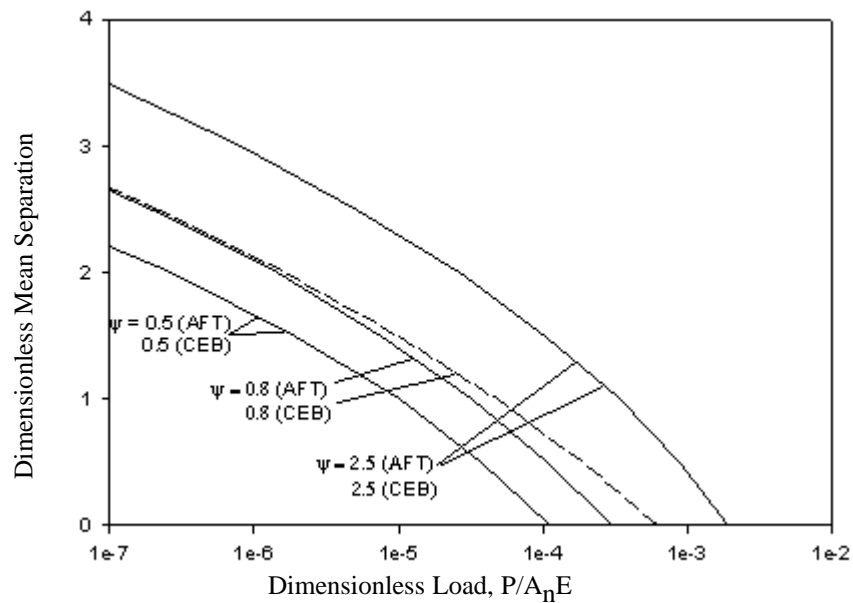


Figure 5. Dimensionless separation versus contact load: Comparison between AFT and CEB models

Table 1. Plasticity index and surface topography

$\Psi$	$\eta R \sigma$	$\sigma/R$	$\sigma/\sigma_s$
0.5	0.0302	$8.75 \times 10^{-5}$	1.299192
0.8	0.374	$2.00 \times 10^{-4}$	1.001331
2.5	0.601	$1.77 \times 10^{-3}$	1.000515

separation  $h^*$  versus dimensionless load  $\frac{P}{A_n E}$  for different values of plasticity index,  $\phi$ , as predicted by the AFM and CEB models. It is clear from the figure that the separation increases with the plasticity index for a given load. For low plasticity index (harder material), the contact is approximately totally elastic. As summarized in Table 1, lower plasticity index corresponds to larger critical interference,  $w_c$ . This, in turn, increases effective separation for plastic asperity as seen in Eqs. (32) and (33). The result is diminished contributions of plastic asperities. Hence, in Eq. (30)  $P_{e2}$  and  $P_{p2}$  attain smaller values, resulting in the following approximation:

$$P^*(h^*) = P_{e1}^* \quad (38)$$

Therefore material with low plasticity index may be approximated as a purely elastic body. On the other hand, for high plasticity index (softer material), the contact is approximately totally plastic and the total expected dimensionless contact load for elastic-plastic contact of Eq. (30) is approximately:

$$P^*(h^*) = P_{p2}^* \quad (39)$$

Figure 6 depicts the contact area ratio versus dimensionless contact load for different values of  $\phi$ , as predicted by the AFM and CEB models.

#### 4.2 Comparison of AFM, CEB and KKPK models

It is the intent of this subsection to evaluate the proposed model (AFT) and present a comparative study of the model with those proposed by CEB and KKPK. In doing so we present the experimental results by Kucharski et al. (1994) as the basis of these comparisons. They presented a finite element model of elastic-plastic contact (referred to as KKPK). They also performed measurement of contact load, area and approach. In their work, steel specimens are employed with Young's modulus  $E_1 = 200,000$  MPa, Poisson's ratio  $\nu_1 = 0.3$  and tensile yield strength  $Y = 400$  MPa. The three dimensional profilometry of sand-blasted surface (E60), average over three samples, are given as follows Kucharski et al. (1994):

- Areal summit density  $\eta = 655.4 \text{ mm}^{-2}$
- Mean summit radius  $R = 30.0 \mu\text{m}$
- 3D standard deviation of summit height distribution  $\sigma = 2.3 \mu\text{m}$
- 3D maximum peak height  $z_{max} = 13.5 \mu\text{m}$
- 3D standard deviation of the surface height distribution  $\sigma_s = 2.95 \mu\text{m}$
- 3D maximum summit height  $M_{sh} = 9.9 \mu\text{m}$

As in Kucharski *et al.* (1994),  $3Y/2$  is employed instead of  $KH$  value in calculating the plastic contact contribution. Moreover, dimensionless approach is used instead of separation in presenting the results. In this case,

approach is obtained by Kucharski et al. (1994):

$$a = z_{max} - h \quad (40)$$

where  $\alpha$  is the approach, and  $z_{max}$  and  $h$  are the maximum peak height and separation.

Figure 7 illustrates the results. In this case dimensionless approach is with respect to the maximum summit height,  $M_{sh}$ . Clearly, the proposed (AFM) model presents the most favorable agreement between the predicted contact load/approach values to that obtained by measurements. The accuracy of the AFM model is also attested to by the results shown in Fig. 8. The results show that the AFM model provides significantly more accurate prediction of contact load and contact area than CEB and KKPK models.

#### 4.3 Elastic-Plastic Contact for Rough Surfaces

In this section direct formulation of contact of rough-on-rough surfaces based on the work of Greenwood and Tripp (1967) is presented. The purpose here is to demonstrate the adaptability of the proposed contact model using plastic asperity concept and also a formal mathematical treatment of contact between two rough surfaces. Greenwood and Tripp (1967) introduced elastic as well as plastic models for two rough surfaces covered with paraboloidal asperities. Consideration of contact between two asperities results in the following description of interference

$$w = z_1 + z_2 - 2f(r/2) \quad (41)$$

where  $z_1$  and  $z_2$  are the heights of asperities on surfaces one and two, respectively.  $r$  is the radial distance denoting the offset between the central lines of the two asperities. For a summit radius of curvature  $R$ , the presumption of Hertzian contact leads to:

$$A_0 = \pi \frac{R}{2} w \quad (42)$$

$$P_0 = \frac{4}{3} E \left( \frac{R}{2} \right)^{1/2} w^{3/2} \quad (43)$$

The expected dimensionless contact load for elastic contact is

$$P^*(h^*) = \left( \frac{16\sqrt{2}}{15} \right) \pi \beta^2 \sqrt{\frac{\sigma}{R}} F_{5/2}(h^* - y_s^*) \quad (44)$$

and that for plastic contact is

$$P^*(h^*) = 2\pi^2 \beta^2 \frac{H}{E} F_2(h^* - y_s^*) \quad (45)$$

where,

$$F_n(u) = \int_u^\infty (s-u)^n \phi(s) ds$$

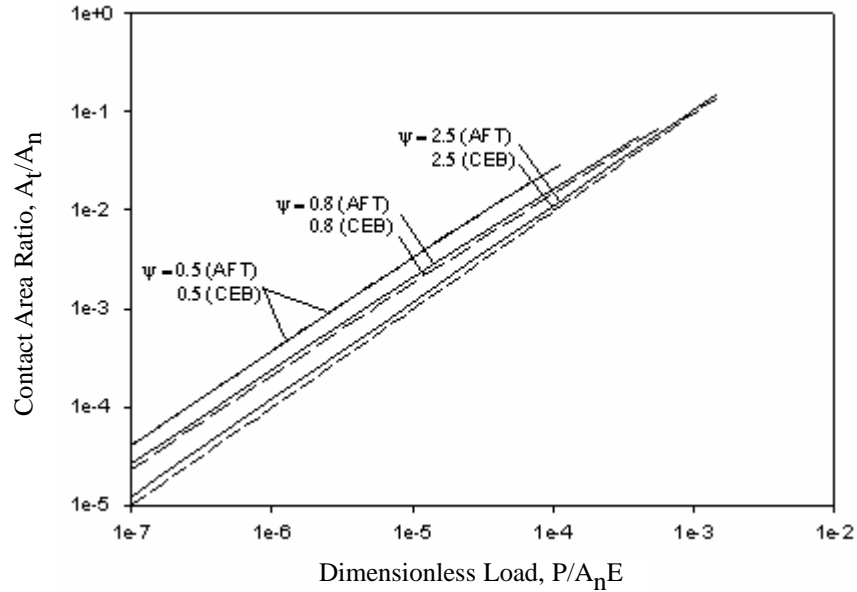


Figure 6. Contact area ratio versus contact load: Comparison between AFT and CEB models

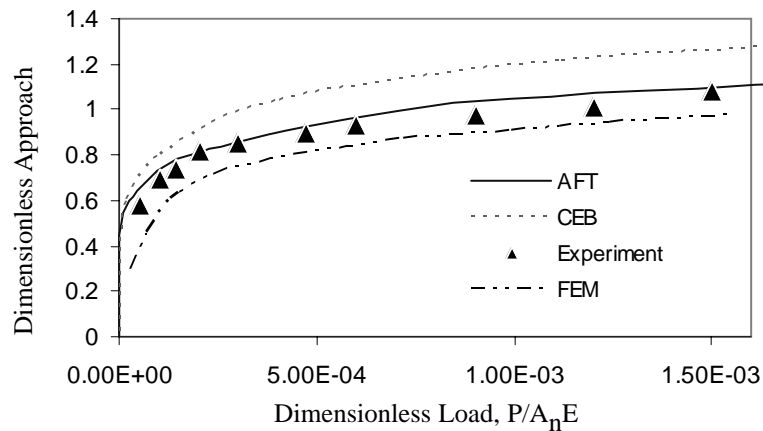


Figure 7. Contact load versus approach: Comparison between AFT, CEB, experimental results of KKPK, and FEM model of KKPK

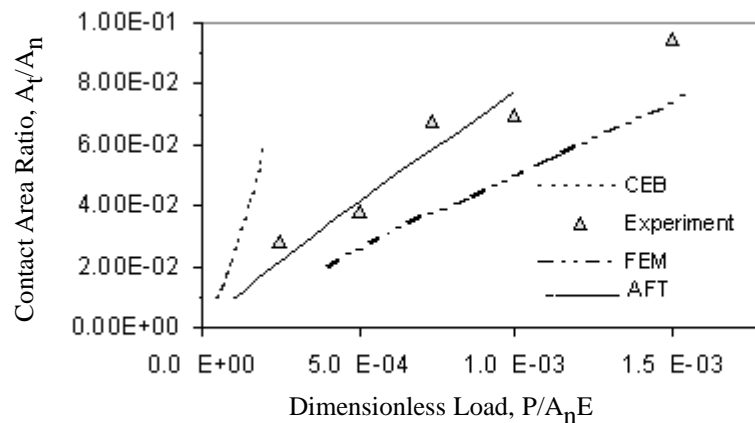


Figure 8. Contact area versus dimensionless load: Comparison between AFT, CEB, experimental results of KKPK, and FEM model of KKPK

Hence, using the proposed method, the total dimensionless expected contact load for elastic-plastic behavior is:

$$P_t^*(h^*) = P_{e1}^* + P_{p2}^* - P_{e2}^* \quad (46)$$

where,

$$P_{e1}^*(h^*) = \left( \frac{16\sqrt{2}}{15} \right) \pi \beta^2 \sqrt{\frac{\sigma}{R}} F_{5/2}(h^* - y_s^*) \quad (47)$$

$$P_{e2}^* = \left( \frac{16\sqrt{2}}{15} \right) \pi \beta_p^2 \sqrt{\frac{\sigma}{R}} F_{5/2}(h^* - y_s^* + w_c^*) \quad (48)$$

$$P_{p2}^* = 2\pi^2 \beta_p^2 \frac{H}{E} F_2(h^* - y_s^* + w_c^*) \quad (49)$$

and  $\sigma$  denotes the standard deviation of sum of asperity heights on the two surfaces.

## 5. Conclusions

A mathematical formulation of elastic-plastic contact has been presented in this paper. Using the definition of critical interference, the concept of elastic and plastic asperities have been developed in which a rough surface is represented by two surfaces. The first surface is the actual physical surface and is assumed to deform as a purely elastic body. The second surface is a fictitious one and it is derived from the physical surface and the critical interference. This surface is assumed to deform as a purely plastic body. The development of the elastic and plastic surfaces has facilitated the mathematical formulation of elastic-plastic contact of rough surfaces. Comparison of the proposed model with the existing models for elastic-plastic contact have been performed. The measurement results of previously performed experiments on sand-blasted steel surface (Kucharski *et al.* 1994) have shown that the proposed model provides significant improvement over previous models in the prediction of contact load and area of contact. The proposed model (AFT) gives better prediction than CEB since in CEB for every asperity the elastic quantity due to plastic pressure  $Q_{e2}$  is not considered. Hence, the elastic and plastic behaviors do not occur simultaneously for an asperity. Therefore, their formulation can only be characterized as an elastic-then-plastic model at microscopic scale and elastic-plastic model at macroscopic scale.

## Appendix A

Consider an asperity and assume that its shape is quadratic as proposed by Greenwood and Tripp (1971). The equation of the surface asperity is given by

$$y = \frac{1}{2R} \rho^2 \quad (A1)$$

as shown in Fig. 2. The figure also illustrates fictitious plastic asperity whose shape is obtained by a displacement of  $w_c$  along the normal to the quadratic curve. Let  $\bar{u}_t$  and  $\bar{u}_n$  represent the tangential and normal unit vector to the quadratic at point A. The position of point A is given by vector  $\bar{r}_A$  as:

$$\bar{r}_A = \rho \bar{i} + y \bar{j} = \rho \bar{i} + \frac{\rho^2}{2R} \bar{j} \quad (A2)$$

The unit tangential vector is obtained as

$$\bar{u}_t = \frac{d\bar{r}_A}{|d\bar{r}_A|} = \frac{1}{\sqrt{1 + \frac{\rho^2}{R^2}}} (\bar{i} + \frac{\rho}{R} \bar{j}) \quad (A3)$$

Hence the unit normal vector is

$$\bar{u}_n = \frac{1}{\sqrt{1 + \frac{\rho^2}{R^2}}} (-\frac{\rho}{R} \bar{i} + \bar{j}) \quad (A4)$$

Then the description of the plastic asperity is obtained by

$$\bar{r}_B = \bar{r}_A + w_c \bar{u}_n - w_c \bar{j} \quad (A5)$$

or

$$\bar{r}_B = \rho \left( 1 - \frac{w_c}{R} \right) \bar{i} + \left( \frac{\rho^2}{2R} + \frac{w_c}{\sqrt{1 + \frac{\rho^2}{R^2}}} - w_c \right) \bar{j} \quad (A6)$$

For small  $\frac{w_c}{R}$  and  $\frac{\rho}{R}$ ,  $\bar{r}_B$  may be approximated by:

$$\bar{r}_B = \rho \left( 1 - \frac{w_c}{R} \right) \bar{i} + \frac{\rho^2}{2R} \left( 1 - \frac{w_c}{R} \right) \bar{j} \quad (A7)$$

let

$$x = \rho \left( 1 - \frac{w_c}{R} \right)$$

then

$$\bar{r}_B = x \bar{i} + \frac{x^2}{2(R - w_c)} \bar{j} \quad (A8)$$

Therefore, the shape of the plastic (fictitious) asperity is given by:

$$y = \frac{x^2}{2(R - w_c)} \quad (A9)$$

## References

- Abbott, E. J. and Firestone, F.A., 1933, "Specifying Surface Quantity-Method Based on Accurate Measurement and Comparison," *Mech. Engr.* Vol. 55, pp. 569-577.
- Bush, A. W., Gibson, R. D. and Thomas, T. R., 1975, "The Elastic Contact of a Rough Surface," *Wear*, Vol. 35, pp. 87-111.
- Chang, W.R., 1997, "An Elastic-Plastic Contact Model for a Rough Surface with an Ion-Plated Soft Metallic Coating," *Wear*, Vol. 212, pp. 229-237.
- Chang, W.R., Etsion, I. and Bogy, D.B., 1986, "An Elastic-Plastic Model for the Contact of Rough Surfaces," *J. of Tribology*, Vol. 109, pp. 257-263.
- Francis, H. A., 1977, "Application of Spherical Indentation Mechanics to Reversible and Irreversible Contact between Rough Surfaces," *Wear*, Vol. 45, pp. 221-269.
- Francis, H. A., 1976, "Phenomenological Analysis of Plastic Spherical Indentation," *ASME J. of Engineering Materials and Technology*, Vol. 98, pp. 272-281.
- Greenwood, J. A. and Williamson, J. B. P., 1966, "Contact of Nominally Flat Surfaces," *Proc. Roy. Soc. (London)* Vol. A295, pp. 300-319.
- Greenwood, J. A. and Tripp, J. H., 1967, "The Elastic Contact of Rough Sphere," *ASME J. of Appl.* Vol. 34, pp. 153-159.
- Greenwood, J. A. and Tripp, J. H., 1970, "The Contact of Two Rough Nominally Flat Rough Surfaces," *Proc. Instn. Mech. Engrs.* Vol. 185, pp. 625-633.
- Hisakado, T., 1974, "Effect of Surface Roughness on Contact Between Solid Surfaces," *Wear*, Vol. 28, pp. 217-234.
- Hornig, J. H., 1998, "An Elliptic Elastic-Plastic Aspiration Microcontact Model for Rough Surfaces," *ASME J. of Tribology*, Vol. 120, pp. 82-88.
- Ishigaki, H., Kawaguchi, I. and Mizuta, S., 1979, "A Simple Estimation of the Elastic-Plastic Deformation of Contacting Asperities," *Wear*, Vol. 54, pp. 157-164.
- Kogu, L. and Etsion, I., 2002, "Elastic-Plastic Contact Analysis of a Sphere and a Rigid Flat," *ASME J. of Appl. Mech.* Vol. 69, pp. 657-662.
- Kogu, L. and Etsion, I., 2003, "A Finite Element Based Elastic - Plastic Model for the Contact of Rough Surfaces," *Trib. Trans.* pp. 383-390.
- Kucharski, S., Klimczak, T., Polijaniuk, A. and Kaczmarek, J., 1994, "Finite-Element Model for the Contact of Rough Surfaces," *Wear*, Vol. 177, pp. 1-13.
- Liu, Z., Neville, A. and Reuben, R. L., 2000, "An Analytical Solution for Elastic and Elastic-Plastic Contact Models," *ASME J. of Tribology*, Vol. 43, pp. 627-633.
- Liu, G., Zhu, J.L., Yu, L. and Wang, Q.J., 2001, "Elastic-Plastic Contact of Rough Surfaces," *ASME J. of Tribology*, Vol. 44, pp. 437-443.
- McCool, J. I., 1986, "Predicting Microfracture in Ceramics Via a Microcontact Model," *ASME J. of Tribology*, Vol. 108, pp. 380-386.
- Nayak, P. R., 1973, "Random Process Model of Rough Surfaces in Plastic Contact," *Wear*, Vol. 26, 305-333.
- Nayak, P. R., 1971, "Random Process Model of Rough Surfaces," *ASME J. of Lubrication Technology*, Vol. 93, pp. 398-407.
- Nuri, K. A. and Halling, J., 1975, "The Normal Approach between Rough Flat Surfaces in Contact," *Wear*, Vol. 32, pp. 81-93.
- Pullen J. and Williamson, J.B.P., 1972, "On the Plastic Contact of Rough Surfaces," *Proc. Roy. Soc (London)*, Vol. A327, pp. 159-173.
- Tabor, D.J., 1977, "Collide Interface Science," *Proc. Roy. Soc (London)*, Vol. 58(2), pp. 2-10.